Achievable Rate Region of Non-Orthogonal Multiple Access Systems with Wireless Powered Decoder

Jie Gong *Member, IEEE*, Xiang Chen *Member, IEEE*

arXiv:1703.03179v1 [cs.IT] 9 Mar 2017

Abstract

Non-orthogonal multiple access (NOMA) is a candidate multiple access scheme in 5G systems for the simultaneous access of tremendous number of wireless nodes. On the other hand, RF-enabled wireless energy harvesting is a promising technology for self-sustainable wireless nodes. In this paper, we consider a NOMA system where the near user harvests energy from the strong radio signal to power-on the information decoder. A generalized energy harvesting scheme is proposed by combining the conventional time switching and power splitting scheme. The achievable rate region of the proposed scheme is characterized under both constant and dynamic decoding power consumption models. If the decoding power is constant, the achievable rate region can be found by solving two convex optimization subproblems, and the regions for two special cases: time switching and power splitting, are characterized in closed-form. If the decoding power is proportional to data rate, the achievable rate region can be found by exhaustive search algorithm. Numerical results show that the achievable rate region of the proposed generalized scheme is larger than those of time switching scheme and power splitting scheme, and rate-dependent decoder design helps to enlarge the achievable rate region.

I. Introduction

With the tremendous increase of mobile users for high-speed video service and machine-type communication nodes for Internet-of-Things (IoT) applications in the coming years, the

Jie Gong is with Guangdong Key Laboratory of Information Security Technology, School of Data and Computer Science, Sun Yat-sen University, Guangzhou 510006, Guangdong, China. Email: gongj26@mail.sysu.edu.cn.

Xiang Chen is with School of Electronics and Information Engineering, SYSU-CMU Shunde International Joint Research Institute, Sun Yat-Sen University, Guangzhou 510006, China. He is also with Key Lab of EDA, Research Institute of Tsinghua University in Shenzhen, Shenzhen 518057, China. Email: chenxiang@mail.sysu.edu.cn.

next generation mobile communication systems (5G) will encounter severe scarcity of radio resources. Non-orthogonal multiple access (NOMA), in which the users access the network in the same frequency band and are distinguished in the power domain, is expected as one of the candidate solutions to greatly enhance the spectrum efficiency [1]. The basic idea of NOMA (as proposed in [2]) is that two users, a far user and a near user, access in the same frequency band, and are allocated with higher and lower transmit power, respectively. The far user directly decodes its desired information, while the near user adopts successive interference cancellation (SIC) to firstly decode and subtract the information of the far user, and then decode the desired information for itself. Inspired by the fact that the near user receives very strong radio signal, it is promising to apply RF-enabled wireless energy harvesting technology for this near user, which facilitates the application of self-sustain devices in the IoT networks [3], such as sensor nodes and RFIDs.

NOMA has been extensively studied in the literature. Saito, et. al [2] firstly proposed the concept for 5G, and system-level performance evaluation was done in [4], showing that both the network capacity and the cell-edge user throughput can be improved compared with the conventional orthogonal multiple access. Uplink NOMA was considered in [5], in which a novel subcarrier and power allocation algorithm was proposed to maximize the users' sum-rate. Taking user fairness into account, the power allocation problem was studied in [6]. In multiuser scenario, user pairing was taken into account in [7], and its impact on the performance was characterized. Further, since near user can decode the information of far user, the authors in [8] proposed a cooperative NOMA scheme, in which the near user serves as a relay to help the far user. The work was further extended to combine simultaneous wireless information and power transfer (SWIPT) [9]. However, the previous work only considers transmit power consumption. In fact, the receiving circuit power consumption cannot be ignored in applications such as wireless sensors [10]. Specifically, in NOMA system, SIC receiver adopted at the near user consumes more energy than conventional receivers. A constant receiver power consumption with ambient energy source is considered in [11], which provides an intuition on how to efficiently allocate the harvested energy. Nevertheless, as wireless radio energy is controllable compared with ambient energy, how to allocate the received signal between energy harvesting and information decoding depending on the receiver power consumption is an open problem.

In fact, two types of receiver structures, power splitting receiver [12] and time switching receiver [13], have been proposed for the RF-enabled wireless energy harvesting. The research

on SWIPT further extends to MIMO broadcasting channel [14], multiuser OFDM systems [15], relay networks [16], and cellular network [17]. Since the receiver can harvest energy from both desired signal and interference, strong interference will benefit wireless energy harvesting. Based on this, two-user interference channel and multi-user interference channel were studied in [18] and [19], respectively. However, most of the previous works mainly focus on characterizing the rate-energy tradeoff by adjusting the portion of received signal on energy harvesting and information decoding. Again, the harvested energy is mainly used for data transmission rather than receiving.

In this paper, we study a NOMA system composed of a base station (BS) and two users, where the near user is self-powered by wireless energy harvesting. It splits the received radio signal into two parts for energy harvesting and information decoding, respectively. The harvested energy is used to power-up the information decoding module. We aim to characterize the achievable rate region (R_1, R_2) of the near user (with rate R_1) and the far user (with rate R_2). A generalized energy harvesting scheme based on the conventional time switching and power splitting is proposed. To find the achievable rate region, we formulate a problem to maximize the achievable rate of UE 2 given the target rate of UE 1. The problem is solved under both constant and dynamic decoding power assumptions. With constant decoding power consumption, two special cases, time switching scheme and power splitting scheme, are firstly studied and closed-form solution is obtained. Then the analysis is extended to the generalized scheme, where the rate maximization is a convex optimization problem, and hence can be efficiently solved by a numerical search algorithm. Numerical results show that the proposed generalized scheme achieves a larger rate region compared with conventional time switching and power splitting scheme. With dynamic decoding power consumption, the optimal solution is found via an exhaustive search algorithm, and the achievable rate regions with different power consumption are analyzed.

The primary contributions of this paper are summarized as follows.

- A generalized energy harvesting scheme is proposed by combining time switching scheme and power splitting scheme. A rate maximization problem is formulated to maximize the achievable rate of UE 2 under the constraint of UE 1's target rate. The boundary of the achievable rate region of the NOMA system can be obtained by solving this problem.
- With constant decoding power consumption, the boundaries of the achievable rate regions for time switching scheme and power splitting scheme are characterized in closed-form. For time switching scheme, there exists a *cut-off* line one the rate region. The rate pairs on

the right side of this cut-off line are not achievable. For power splitting scheme, there is a stringent feasibility requirement on the channel quality of UE 1.

- The boundary of the achievable rate region form the generalized scheme with constant decoding power consumption can be obtained by solving two convex optimization subproblems. It is proved that the optimal solution is the most *economical* one, i.e., the harvested energy is equal to the information decoding power consumption. It is also shown that the generalized scheme has a larger rate region compared with the conventional schemes.
- With dynamic decoding power consumption, an efficient exhaustive search algorithm is proposed to find the boundary of the achievable rate region. Numerical results show that by trading rate with power consumption, the rate region can be greatly extended compared with constant power model.

The rest of the paper is organized as follows. Section II describes the system model and the problem formulation. The problems under constant and dynamic decoding power assumption are analyzed in Sections III and IV, respectively. Extensive results and discussions are presented in Section V. Finally, Section VI concludes the paper.

II. System Model and Problem Formulation

We consider a downlink wireless communication system as shown in Fig. 1, where the BS serves a near user (UE 1) and a far user (UE 2) in the same frequency band. Power domain NOMA scheme is applied in this system, i.e., the BS simultaneously transmits data to both users by superposition coding with different power levels. After receiving the coded signal, UE 2 directly decodes its desired information by viewing the interference from UE 1 as noise. On the other hand, UE 1 applies SIC scheme to enhance its performance by firstly decoding and removing the interference signal of UE 2, and then decoding the desired signal of UE 1. By adjusting the power allocation between two users, per-user throughput can be flexibly controlled. UE 1 is also equipped with an energy harvester, in which the energy carried in the radio signal is harvested to power-on the signal receiving and decoding module.

A. Signal Model

The desired signal for UE $i(i = 1, 2)$ is denoted by x_i with mean $\mathbb{E}[|x_i|^2] = 1$. The superposition coded signal can be represented as

$$x = \sqrt{P_1}x_1 + \sqrt{P_2}x_2, \tag{1}$$

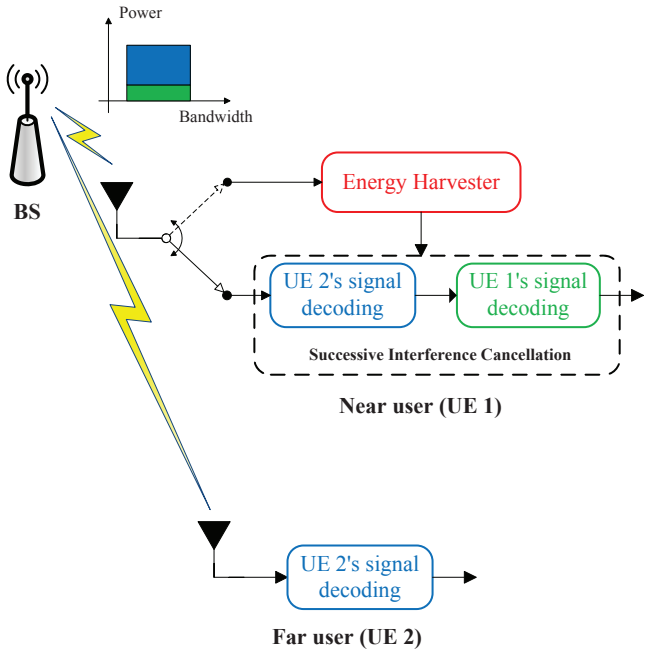

Fig. 1. A NOMA system with wireless powered SIC decoder.

where $P_i, (i = 1, 2)$ is the transmit power for UE i. The total power budget is denoted by $P_{\max}$. The received signal at UE i is

$$\begin{aligned} y_i &= h_i x + n, \\ &= h_i \sqrt{P_1} x_1 + h_i \sqrt{P_2} x_2 + n, \quad i = 1, 2, \end{aligned} \tag{2}$$

where h_i is the channel coefficient from the BS to UE i, n is the additive white Gaussian noise (AWGN) with zero mean and variance σ^2. And we assume $\frac{|h_1|^2}{\sigma^2} > \frac{|h_2|^2}{\sigma^2}$, and the link quality $|h_1|^2$ is good enough so that UE 1 can be self-powered on by energy harvesting.

B. Energy Harvesting Scheme and Constraints

A generalized scheme for energy harvester design is proposed in this paper, which combines the conventional time switching scheme and power splitting scheme. Specifically, each transmission slot is divided into two sub-slots. In the first sub-slot, UE 1 works as a *pure* energy harvester and only the information for UE 2 is carried in the radio signal. Denote $P_1^{(1)}$ and $P_2^{(1)}$ as the power allocation in the first sub-slot. We have $P_1^{(1)} = 0$ and

$$P_2^{(1)} \leq P_{\max}. \tag{3}$$

According to the Shannon's capacity theorem, the achievable rate of UE 2 in the first sub-slot can not exceed the channel capacity, i.e.,

$$R_2^{(1)} \leq \log_2\Big(1+\frac{|h_2|^2 P_2^{(1)}}{\sigma^2}\Big). \tag{4}$$

In the second sub-slot, UE 1 adopts power splitting scheme, i.e., a portion of signal power, denoted by $\rho(0 \leq \rho \leq 1)$, is split to energy harvester, and the other portion, denoted by $1-\rho$, is split to information decoder. Denote $P_1^{(2)}$ and $P_2^{(2)}$ as the power allocation in the second sub-slot. Under the total power constraint

$$P_1^{(2)} + P_2^{(2)} \leq P_{\max}, \tag{5}$$

the desired signal power for UE 1 is $(1-\rho)P_1^{(2)}$. Since the interference can be completely eliminated by SIC, UE 1 can be viewed as an interference-free receiver. Hence, its achievable rate satisfies

$$R_1^{(2)} \leq \log_2\Big(1+\frac{|h_1|^2(1-\rho)P_1^{(2)}}{\sigma^2}\Big). \tag{6}$$

UE 2 decodes its desired signal by viewing the interference from UE 1 as noise. The achievable rate is constrained by

$$R_2^{(2)} \leq \log_2\Big(1+\frac{|h_2|^2 P_2^{(2)}}{|h_2|^2 P_1^{(2)}+\sigma^2}\Big). \tag{7}$$

In addition, to guarantee that SIC scheme works, UE 1 should be able to successfully decode the data for UE 2. Thus, besides (7), $R_2^{(2)}$ is also constrained by the decoding ability of UE 1, i.e.,

$$R_2^{(2)} \leq \log_2\Big(1+\frac{|h_1|^2(1-\rho)P_2^{(2)}}{|h_1|^2(1-\rho)P_1^{(2)}+\sigma^2}\Big). \tag{8}$$

Without loss of generality, we assume the slot length is normalized to 1. Denote the length of the first sub-slot by $t(0 \leq t \leq 1)$, and that of the second sub-slot by $1-t$. The total harvested energy should be no smaller than the required energy for information decoding, i.e.,

$$t\xi|h_1|^2 P_2^{(1)} + (1-t)\rho\xi|h_1|^2(P_1^{(2)}+P_2^{(2)}) \geq (1-t)P_{\mathrm{SIC}}, \tag{9}$$

where $0<\xi<1$ is the energy harvesting efficiency, and P_{SIC} is the total power consumption for information decoding.

Notice that the conventional time switching scheme can be viewed as a special case of the generalized scheme with $\rho=0$, and the conventional power splitting scheme is a special case with $t=0$. Later, we will extensively study generalized scheme as well as time switching scheme and power splitting scheme.

C. Problem Formulation

In this paper, we aim to characterize the achievable rate regions of UE 1 and UE 2 under the proposed schemes, which can be represented as

$$\begin{aligned}\mathcal{R} = \{(R_1, R_2) \big| & R_1 = (1-t)R_1^{(2)}, R_2 = tR_2^{(1)} + (1-t)R_2^{(2)}, \\ & 0 \le t \le 1, 0 \le \rho \le 1, R_2^{(1)}, P_2^{(1)}, R_1^{(2)}, R_2^{(2)}, P_1^{(2)}, P_2^{(2)} \text{ satisfy (3)-(9)}\},\end{aligned} \tag{10}$$

where all the variables are nonnegative. The achievable rate region can be described by the boundary curve which maps each feasible R_1 to the maximum of R_2. Thus, the boundary curve of the achievable rate region (10) can be found by maximizing R_2 for all the given R_1, which is formulated as

$$(\mathbf{P0}) \quad \max \ tR_2^{(1)} + (1-t)R_2^{(2)} \tag{11a}$$

$$\text{s.t.} \ (1-t)R_1^{(2)} = r, \tag{11b}$$

$$0 \le t < 1, 0 \le \rho < 1, \tag{11c}$$

$$(3)\text{-}(9),$$

where $r > 0$ is the target average rate of UE 1, and the optimization variables include t, ρ, $R_2^{(1)}$, $P_2^{(1)}$, $R_1^{(2)}$, $R_2^{(2)}$, $P_1^{(2)}$, and $P_2^{(2)}$. Notice that $r > 0$ means that only the cases with nonzero achievable rate for UE 1 are considered. In this sense, it can be easily found that $t \neq 1$ and $\rho \neq 1$ according to (11b). Thus, we have $t < 1$ and $\rho < 1$ as in (11c) so that the terms $\frac{1}{1-t}$ and $\frac{1}{1-\rho}$ that appear in the following contents are well defined.

In reality, the information decoding power consumption P_{SIC} can be modeled either constant or dynamic based on receiver circuit structure and decoding scheme. In the following sections, we will solve the problem $(\mathbf{P0})$ under different power consumption models.

III. Constant Decoding Power Consumption Case

In this section, we characterize the achievable rate region with constant power consumption model. This model has been widely used in the literature and well models the iterative decoding scheme with fixed number of iterations in real system. In addition, well-structured results can be obtained based on this model as shown later. These results can help us to better understand the relation between parameters and performance, and provide inspiring intuitions for the design of real systems.

Specifically, we assume $P_{\rm SIC}$ is constant. At first, some quick observations on the problem ($\mathbf{P0}$) are summarized as follows.

Lemma 1. ***(Equality Constraints)*** *To achieve the maximum of the problem ($\mathbf{P0}$), the constraints (3), (4), (5), (6) and (7) (or (8)) are satisfied with equality.*

Proof. See Appendix A. □

Lemma 2. ***(Constraint on*** R_2***)*** *If*

$$|h_2|^2 \leq (1-\rho)|h_1|^2, \tag{12}$$

R_2 *is constrained by (7). Otherwise, it is constrained by (8).*

Proof. The lemma is proved by directly comparing the right hand sides of (7) and (8). □

Based on Lemmas 1 and 2, all the optimization variables can be represented in terms of t and ρ, and the problem formulation can be simplified. To start with, we firstly consider two special cases: time switching scheme and power splitting scheme, where there is only a single variable t or ρ. Then the analysis is extended to the generalized scheme.

A. Time Switching Scheme

Recall that time switching scheme is a special case of the generalized scheme with $\rho = 0$. In this case, we always have $|h_2|^2 \leq (1-\rho)|h_1|^2$, and hence, R_2 is constrained by (7), and the power constraint degrades to

$$t\xi|h_1|^2 P_{\max} \geq (1-t)P_{\rm SIC}. \tag{13}$$

As the constraints (3)-(7) are all satisfied with equality, by simple calculation, the problem ($\mathbf{P0}$) can be reformulated with a single variable t as

$$(\mathbf{P1}) \quad \max_{t} \ f_0(t) \tag{14a}$$

$$\text{s.t.} \ \frac{P_{\rm SIC}}{\xi|h_1|^2 P_{\max} + P_{\rm SIC}} \leq t \leq 1 - \frac{r}{\log_2\left(1+\frac{|h_1|^2 P_{\max}}{\sigma^2}\right)}, \tag{14b}$$

where the objective function is

$$f_0(t) = \log_2\left(1+\frac{|h_2|^2 P_{\max}}{\sigma^2}\right) - (1-t)\log_2\left(\frac{|h_2|^2}{|h_1|^2}\left(2^{\frac{r}{1-t}}-1\right)+1\right), \tag{15}$$

the left inequality of (14b) is derived from (13), and the right inequality of (14b) holds as $r = (1-t)\log_2(1+\frac{|h_1|^2P_1^{(2)}}{\sigma^2}) \leq (1-t)\log_2(1+\frac{|h_1|^2P_{\max}}{\sigma^2})$. We have the following lemma.

Lemma 3. ***(Monotonicity)*** *The function $f_0(t)$ is non-increasing for $0 \leq t < 1$.*

Proof. See Appendix B. □

Based on Lemma 3, the optimal solution of problem ($\mathbf{P1}$) can be directly obtained by taking the minimum value of t. We summarize the result in the following theorem.

Theorem 1. *The optimal solution for the problem ($\mathbf{P1}$) is*

$$R_{2,\mathrm{TS}}^* = \log_2\left(1+\frac{|h_2|^2P_{\max}}{\sigma^2}\right) - \frac{\xi|h_1|^2P_{\max}}{\xi|h_1|^2P_{\max}+P_{\mathrm{SIC}}}\log_2\left(\frac{|h_2|^2}{|h_1|^2}\left(2^{\frac{r(\xi|h_1|^2P_{\max}+P_{\mathrm{SIC}})}{\xi|h_1|^2P_{\max}}}-1\right)+1\right), \tag{16}$$

which is achieved when

$$t = \frac{P_{\mathrm{SIC}}}{\xi|h_1|^2P_{\max}+P_{\mathrm{SIC}}}. \tag{17}$$

The feasible region of r is

$$0 \leq r \leq \frac{\xi|h_1|^2P_{\max}}{\xi|h_1|^2P_{\max}+P_{\mathrm{SIC}}}\log_2\left(1+\frac{|h_1|^2P_{\max}}{\sigma^2}\right). \tag{18}$$

In Theorem 1, the feasible region of r is obtained by guaranteeing that the feasible region of t defined by (14b) is nonempty. Notice that when (17) holds, (13) is satisfied with equality. That is, Theorem 1 holds as the amount of harvested energy equals to the required energy for information decoding, which intuitively, is the most *economical* way of dividing the received signal between energy harvesting and information decoding.

Based on Theorem 1, we have the following corollary.

Corollary 1. *For all r satisfying (18), we have*

$$\frac{P_{\mathrm{SIC}}}{\xi|h_1|^2P_{\max}+P_{\mathrm{SIC}}}R_{2,\max} \leq R_{2,\mathrm{TS}}^* \leq R_{2,\max}, \tag{19}$$

where $R_{2,\max} = \log_2\left(1+\frac{|h_2|^2P_{\max}}{\sigma^2}\right)$

Corollary 1 tells us that when $R_1 = 0$, $R_{2,\mathrm{TS}}^*$ achieves its maximum, i.e., all the power resource is allocated to UE 2. However, when R_1 equals to the right hand side of (18), $R_{2,\mathrm{TS}}^*$ achieves its minimum, which is strictly larger than 0. It means that there is a *cut-off* line on achievable rate region for time switching scheme. When R_1 achieves the maximal value, we cannot further

increase R_1 by sacrificing R_2. This is due to the nature of time switching: to harvest energy to power-on UE 1, the length of the first sub-slot can never be zero.

B. Power Splitting Scheme

Power splitting scheme is a special case of the generalized scheme with $t = 0$. In this case, the power constraint (9) degrades to

$$\rho\xi|h_1|^2 P_{\max} \geq P_{\text{SIC}}. \tag{20}$$

Based on the above equation, there is a feasibility issue for power splitting scheme, as detailed in the following lemma.

Lemma 4. ***(Feasibility)*** *If*

$$|h_1|^2 \leq \frac{P_{\text{SIC}}}{\xi P_{\max}}, \tag{21}$$

there does not exist any achievable rate pair (R_1, R_2) *in power splitting mode so that* $R_1 > 0$ *and* $R_2 > 0$.

Lemma 4 is directly obtained from (20) as if (21) holds, (20) cannot be satisfied with any feasible value of ρ. According to the above lemma, power splitting scheme is not applicable if the channel of near user is in deep fading.

If $|h_1|^2 \leq \frac{P_{\text{SIC}}}{\xi P_{\max}}$, the problem ($\mathbf{P0}$) is reformulated based on Lemma 1 as

$$(\mathbf{P2}) \quad \max_{\rho} \quad \min\left\{ \log_2\left(\frac{|h_2|^2 P_{\max} + \sigma^2}{|h_2|^2 P_1^{(2)} + \sigma^2}\right), \log_2\left(\frac{|h_1|^2(1-\rho)P_{\max} + \sigma^2}{|h_1|^2(1-\rho)P_1^{(2)} + \sigma^2}\right)\right\} \tag{22a}$$

$$\text{s.t.} \quad \log_2\left(1 + \frac{|h_1|^2(1-\rho)P_1^{(2)}}{\sigma^2}\right) = r, \tag{22b}$$

$$\frac{P_{\text{SIC}}}{\xi|h_1|^2 P_{\max}} \leq \rho < 1, \tag{22c}$$

where $P_1^{(2)}$ in the objective function can actually be represented by ρ based on (22b), and the solution is summarized in the following theorem.

Theorem 2. *If* $|h_1|^2 > \frac{P_{\text{SIC}}}{\xi P_{\max}}$, *the optimal solution for the problem (*$\mathbf{P2}$*) is*

$$R_{2,\text{PS}}^* = \begin{cases} \log_2\left(\frac{(|h_2|^2 P_{\max} + \sigma^2)(\xi|h_1|^2 P_{\max} - P_{\text{SIC}})}{(\xi P_{\max}(|h_2|^2(2^r-1) + |h_1|^2) - P_{\text{SIC}})\sigma^2}\right), & \textit{if } |h_2|^2 \leq |h_1|^2 - \frac{P_{\text{SIC}}}{\xi P_{\max}} \\ \log_2\left(1 + \frac{\xi|h_1|^2 P_{\max} - P_{\text{SIC}}}{\xi\sigma^2}\right) - r, & \textit{else} \end{cases} \tag{23}$$

which is achieved when

$$\rho = \frac{P_{\mathrm{SIC}}}{\xi |h_1|^2 P_{\max}}. \tag{24}$$

The feasible region of r *is*

$$0 \le r \le \log_2 \Big(1 + \frac{\xi |h_1|^2 P_{\max} - P_{\mathrm{SIC}}}{\xi \sigma^2}\Big). \tag{25}$$

Proof. As the objective function in (22a) is a non-increasing function of $P_1^{(2)}$ and ρ, and $P_1^{(2)}$ is an increasing function of ρ, the maximum rate is achieved when $\rho = \frac{P_{\mathrm{SIC}}}{\xi |h_1|^2 P_{\max}}$ and $P_1^{(2)} = \frac{\xi P_{\max}(2^r - 1)\sigma^2}{\xi |h_1|^2 P_{\max} - P_{\mathrm{SIC}}}$. Then the closed-form rate $R_{2,\mathrm{PS}}^*$ is obtained by comparing the two items in the minimization in (22a).

The feasible range of r is obtained according to $0 \le P_1^{(2)} \le P_{\max}$. □

Notice that the optimal is achieved when the harvested energy is equal to the required decoding energy, which is the same with the time switching case. However, the difference is that the power splitting can tradeoff R_1 and R_2 completely. That is, when R_1 gradually decreases to zero, R_2 gradually increases to its maximum, and vise versa. Specifically, when $|h_2|^2 > |h_1|^2 - \frac{P_{\mathrm{SIC}}}{\xi P_{\max}}$, i.e., the channel quality between BS and UE 2 is good enough, R_2 is only constrained by the decoding ability of UE 1, and R_1 trades off with R_2 linearly. However, power splitting scheme has stringent requirement on the channel gain of UE 1 (see Lemma 4). As a result, it is not applicable when the channel of UE 1 is not good enough.

C. Generalized Scheme

Finally, we study the generalized scheme in this section. Based on Lemma 2, the original problem (**P0**) is divided into two subproblems, which are discussed as follows in detail.

1) Subproblem with $|h_2|^2 \le (1-\rho)|h_1|^2$*:* When $|h_2|^2 \le (1-\rho)|h_1|^2$, $R_2^{(2)}$ is equal to the right hand side of (7). By some simple calculation, the problem can be reformulated as

$$(\mathbf{P3.1}) \quad \max_{t,\rho} \ \log_2 \Big(1 + \frac{|h_2|^2 P_{\max}}{\sigma^2}\Big) - (1-t)\log_2 \Big(\frac{|h_2|^2}{(1-\rho)|h_1|^2}\big(2^{\frac{r}{1-t}} - 1\big) + 1\Big) \tag{26a}$$

$$\text{s.t.} \ \ 1 - \rho \ge \frac{|h_2|^2}{|h_1|^2}, \tag{26b}$$

$$(1-t)\log_2 \Big(1 + \frac{|h_1|^2 (1-\rho) P_{\max}}{\sigma^2}\Big) \ge r, \tag{26c}$$

$$\frac{t}{1-t} + \rho \ge \frac{P_{\mathrm{SIC}}}{\xi |h_1|^2 P_{\max}}, \tag{26d}$$

$$0 \le t < 1, 0 \le \rho < 1, \tag{26e}$$

where (26c) comes from the fact that $P_1^{(2)} \leq P_{\max}$, and (26d) is another form of (9). As the objective function in (26a) is a decreasing function of ρ, it is maximized when ρ achieves its minimum, i.e., $\rho = \max\{0, \frac{P_{\rm SIC}}{\xi|h_1|^2 P_{\max}} - \frac{t}{1-t}\}$. Based on the optimal value of ρ, there are two cases as follows.

Case (1.1): If $0 \leq \frac{P_{\rm SIC}}{\xi|h_1|^2 P_{\max}} - \frac{t}{1-t}$, i.e., $t \leq t_U$, where

$$t_U = \frac{P_{\rm SIC}}{P_{\rm SIC} + \xi|h_1|^2 P_{\max}}, \tag{27}$$

we have

$$\rho = \frac{P_{\rm SIC}}{\xi|h_1|^2 P_{\max}} - \frac{t}{1-t}. \tag{28}$$

In this case, (26d) is satisfied with equality, and the problem can be transformed into

$$(\mathbf{P3.1c}) \quad \max_{t} \ f_1(t) \tag{29a}$$

$$\text{s.t.} \ \ f_2(t) \geq r, \tag{29b}$$

$$\max\Big\{0, t_L\Big\} \leq t \leq t_U, \tag{29c}$$

with a single variable t, where the objective function is

$$f_1(t) = \log_2\Big(1 + \frac{|h_2|^2 P_{\max}}{\sigma^2}\Big) - (1-t)\log_2\Big(\frac{|h_2|^2}{|h_1|^2(\frac{1}{1-t} - \frac{P_{\rm SIC}}{\xi|h_1|^2 P_{\max}})}\big(2^{\frac{r}{1-t}} - 1\big) + 1\Big), \tag{30}$$

the constraint function in (29b) is

$$f_2(t) = (1-t)\log_2\Big(1 + \frac{|h_1|^2 P_{\max}}{\sigma^2}\Big(\frac{1}{1-t} - \frac{P_{\rm SIC}}{\xi|h_1|^2 P_{\max}}\Big)\Big), \tag{31}$$

and

$$t_L = 1 - \frac{\xi|h_1|^2 P_{\max}}{P_{\rm SIC} + \xi|h_2|^2 P_{\max}}. \tag{32}$$

The constraint (29c) is obtained from $\frac{|h_2|^2}{|h_1|^2} \leq 1 - \rho \leq 1$ and $0 \leq t < 1$. It can be proved that $f_1(t)$ and $f_2(t)$ are both concave functions.

Lemma 5. ***(Concavity of*** $f_1(t)$***)*** *If* $P_{\rm SIC} < \xi|h_1|^2 P_{\max}$*, the function* $f_1(t)$ *is concave for all* $0 \leq t < 1$*. If* $P_{\rm SIC} \geq \xi|h_1|^2 P_{\max}$*,* $f_1(t)$ *is concave for* $1 - \frac{\xi|h_1|^2 P_{\max}}{P_{\rm SIC}} < t < 1$*.*

Proof. See Appendix C. □

Lemma 6. ***(Concavity of*** $f_2(t)$***)*** *If* $P_{\rm SIC} \leq \xi(|h_1|^2 P_{\max} + \sigma^2)$*, the function* $f_2(t)$ *is concave for* $0 \leq t < 1$*. If* $P_{\rm SIC} > \xi(|h_1|^2 P_{\max} + \sigma^2)$*,* $f_2(t)$ *is concave for* $1 - \frac{\xi|h_1|^2 P_{\max}}{P_{\rm SIC} - \xi\sigma^2} < t < 1$*.*

Proof. By taking the second derivative, we find that

$$f_2''(t) = -\frac{1}{(1-t)^3 \ln 2}\Big(\frac{1}{1-t} - \frac{P_{\rm SIC} - \xi\sigma^2}{\xi|h_1|^2 P_{\max}}\Big)^{-2} \leq 0 \tag{33}$$

holds for both cases. Therefore, the lemma is proved. □

Based on Lemmas 5 and 6, we have the following conclusion.

Theorem 3. *The problem (*$\mathbf{P3.1c}$*) is a convex optimization problem.*

Proof. Since

$$1 - \frac{\xi|h_1|^2 P_{\max}}{P_{\rm SIC} - \xi\sigma^2} < 1 - \frac{\xi|h_1|^2 P_{\max}}{P_{\rm SIC}} < 1 - \frac{\xi|h_1|^2 P_{\max}}{P_{\rm SIC} + \xi|h_2|^2 P_{\max}}, \tag{34}$$

$f_1(t)$ and $f_2(t)$ are all concave functions in the range of t defined by (29c). Hence, the problem ($\mathbf{P3.1c}$) is convex [20, Chap. 4]. □

As ($\mathbf{P3.1c}$) is a convex optimization problem, there exists a unique optimal solution which either satisfies $f_1'(t) = 0$ or is the boundary point defined by (29b)-(29c). However, the equation $f_1'(t) = 0$ is difficult to be directly solved. Instead, by exploring the concavity of the objective and the constraints, the optimal solution can be found by a numerical search algorithm detailed as follows.

Firstly, the feasible set of t is determined according to the constraints (29b) and (29c). Denote $t_1 = \max\{0, t_L\}$, $t_2 = t_U$, we have $t_1 \leq t \leq t_2$. If $f_2(t_1) \geq r$ and $f_2(t_2) \geq r$, the whole set $[t_1, t_2]$ is feasible. Otherwise, there exists at least one value of t satisfying $f_2(t) = r$. If $f_2(t_1) \leq r$ and $f_2(t_2) \geq r$, there is a unique t_3 that satisfies $f_2(t_3) = r$ due to the concavity of $f_2(t)$, which can be found by bisection search method [21, Chap. 2.1]. Thus, the feasible set of t is $[t_3, t_2]$. If $f_2(t_1) \geq r$ and $f_2(t_2) \leq r$ on the other hand, the feasible set is $[t_1, t_3]$, where t_3 is the unique value satisfying $f_2(t_3) = r$. While if $f_2(t_1) \leq r$ and $f_2(t_2) \leq r$, we firstly find any t_0 such that $f_2(t_0) \geq r$, and then find $t_3 \in [t_1, t_0]$ and $t_4 \in [t_0, t_2]$ such that $f_2(t_3) = r$ and $f_2(t_4) = r$. Notice that t_0, t_3 and t_4 can all be found by bisection search. Then the feasible set of t is $[t_3, t_4]$.

Secondly, we search over the feasible set of t to find the optimal value of $f_1(t)$. Given the feasible set of t denoted by $[t_1, t_2]$, if $f_1'(t_1) < 0$, we have $\max_{t\in[t_1,t_2]} f_1(t) = f_1(t_1)$ due to its concavity property. Similarly, if $f_1'(t_2) > 0$, we have $\max_{t\in[t_1,t_2]} f_1(t) = f_1(t_2)$. Otherwise, the optimal solution satisfies $f_1'(t) = 0$, which can be found by bisection search algorithm.

Case (1.2): If $t \geq t_U$ on the other hand, we have $\rho = 0$. Thus, the scheme degrades to time switching, and the rate maximization problem has been solved in Section III-A. According to

Theorem 1, the optimal solution is achieved at the boundary point denoted by (17), which is also included in the problem ($\mathbf{P3.1c}$). Therefore, we have the following conclusion.

Proposition 1. *The problem (*$\mathbf{P3.1}$*) is equivalent to the problem (*$\mathbf{P3.1c}$*).*

2) Subproblem with $|h_2|^2 \geq (1-\rho)|h_1|^2$*:* When $|h_2|^2 \geq (1-\rho)|h_1|^2$, by the same calculation, the problem can be reformulated as

$$(\mathbf{P3.2}) \quad \max_{t,\rho} \ t\log_2\left(1+\frac{|h_2|^2 P_{\max}}{\sigma^2}\right)+(1-t)\log_2\left(1+\frac{|h_1|^2(1-\rho)P_{\max}}{\sigma^2}\right)-r, \tag{35a}$$

$$\text{s.t.} \ \ 1-\rho \leq \frac{|h_2|^2}{|h_1|^2}, \tag{35b}$$

$$\text{(26c)-(26e)}.$$

As the objective function in (35a) is also a decreasing function of ρ, it is maximized when ρ achieves its minimum, which is $\rho = \max\{1-\frac{|h_2|^2}{|h_1|^2}, \frac{P_{\text{SIC}}}{\xi|h_1|^2 P_{\max}} - \frac{t}{1-t}\}$ according to (26d) and (35b). Based on the optimal value of ρ, there are two cases as follows.

Case (2.1): If $1-\frac{|h_2|^2}{|h_1|^2} \leq \frac{P_{\text{SIC}}}{\xi|h_1|^2 P_{\max}} - \frac{t}{1-t}$, i.e., $t \leq t_L$, ρ is expressed as (28), and the problem can be reformulated as

$$(\mathbf{P3.2c}) \quad \max_{t} \ f_3(t) \tag{36a}$$

$$\text{s.t.} \ \ f_2(t) \geq r, \tag{36b}$$

$$1-\frac{\xi|h_1|^2 P_{\max}}{P_{\text{SIC}}} < t \leq t_L, \tag{36c}$$

$$0 \leq t < 1, \tag{36d}$$

where the objective function is

$$f_3(t) = t\log_2\left(1+\frac{|h_2|^2 P_{\max}}{\sigma^2}\right)+f_2(t)-r, \tag{37}$$

and the inequality on the left of (36c) comes from the constraint $\rho < 1$. Notice that the problem ($\mathbf{P3.2c}$) exists only if $t_L \geq 0$, i.e., $|h_2|^2 \geq |h_1|^2 - \frac{P_{\text{SIC}}}{\xi P_{\max}}$. Similar to the problem ($\mathbf{P3.1c}$), the problem ($\mathbf{P3.2c}$) is also convex as shown in the following theorem.

Theorem 4. *The problem (*$\mathbf{P3.2c}$*) is a convex optimization problem.*

Proof. Based on Lemma 6, as

$$1-\frac{\xi|h_1|^2 P_{\max}}{P_{\text{SIC}}-\xi\sigma^2} < 1-\frac{\xi|h_1|^2 P_{\max}}{P_{\text{SIC}}}, \tag{38}$$

the function $f_2(t)$ is concave in the feasible region defined by (36c) and (36d). Hence, the problem ($\mathbf{P3.2c}$) is convex as the objective is maximizing the sum of a linear function and a concave function. □

As the problems ($\mathbf{P3.1c}$) and ($\mathbf{P3.2c}$) are both convex optimization problems and of symmetric problem formulation, the latter can also be solved by the numerical search algorithm proposed in Section III-C1.

Case (2.2): On the other hand, if $t \geq t_L$, we have $\rho = 1 - \frac{|h_2|^2}{|h_1|^2}$, the objective is equal to a constant $R_{2,C} = \log_2\left(1 + \frac{|h_2|^2 P_{\max}}{\sigma^2}\right) - r$. In fact, since the case with $\rho = 1 - \frac{|h_2|^2}{|h_1|^2}$ is also included in the problem ($\mathbf{P3.1}$), we do not need to compare $R_{2,C}$ with the optimal values obtained in other cases.

In summary, the optimal solution for ($\mathbf{P0}$) can be obtained depending on the channel coefficients h_1, h_2 and the target rate of UE 1 $R_1 = r$. If $t_L < 0$, i.e., $|h_2|^2 < |h_1|^2 - \frac{P_{\text{SIC}}}{\xi P_{\max}}$, R_2 is only constrained by the decoding ability of UE 2, and the feasible region of problem ($\mathbf{P3.2c}$) is empty. Hence, the optimal solution of the original problem ($\mathbf{P0}$) is equivalent to that of the subproblem ($\mathbf{P3.1c}$). If $|h_2|^2 \geq |h_1|^2 - \frac{P_{\text{SIC}}}{\xi P_{\max}}$ on the other hand, R_2 is constrained by either the decoding ability of UE 2 or that of UE 1. As a consequence, the optimal solution for ($\mathbf{P0}$) is the maximum between the solution of subproblem ($\mathbf{P3.1c}$) and that of subproblem ($\mathbf{P3.2c}$). The procedure to solve ($\mathbf{P0}$) is detailed in Algorithm 1.

Algorithm 1 Finding Achievable Rate Region for Generalized Scheme

Input: $h_1, h_2, R_1 = r$

Output: R_2

1: **if** $|h_2|^2 < |h_1|^2 - \frac{P_{\text{SIC}}}{\xi P_{\max}}$ **then**
2: Find the optimal solution $R_{2,1}$ of subproblem ($\mathbf{P3.1c}$). Then $R_2 = R_{2,1}$.
3: **else**
4: Find the optimal solution $R_{2,1}$ of subproblem ($\mathbf{P3.1c}$).
5: Find the optimal solution $R_{2,2}$ of subproblem ($\mathbf{P3.2c}$).
6: $R_2 = \max\{R_{2,1}, R_{2,2}\}$.
7: **end if**

Notice that the optimal solution is achieved when (26d) is satisfied equality in both subproblems, which is the same with time switching and power splitting cases. Therefore, the most

economical way of splitting the power is also optimal for the generalized scheme. Also notice that the condition $|h_2|^2 < |h_1|^2 - \frac{P_{\mathrm{SIC}}}{\xi P_{\max}}$ is consistent with the one in theorem 2. It is a novel and critical condition for wireless powered NOMA system. Because part of the received radio power in UE 1 is harvested to power-on the information decoder, the signal power for information decoding is lowered so that in UE 1, the received SINR for UE 2's signal decoding may be lower than that in UE 2. In this case, comparing with the constraint (7) for the conventional NOMA system, the new constraint (8) is more stringent. In consequence, a different objective (with a different expression of $R_2^{(2)}$) is formulated and a new subproblem needs to be solved.

D. Achievable Rate Regions and Discussions

Based on Theorems 1, 2 and Algorithm 1, the achievable regions of time switching scheme, power splitting scheme and generalized scheme can be depicted. In Fig. 2, the parameter settings satisfy $|h_2|^2 < |h_1|^2 - \frac{P_{\mathrm{SIC}}}{\xi P_{\max}}$. It can be seen that the proposed generalized scheme achieves a larger rate region compared with the conventional time switching scheme and power splitting scheme. By observing the colored boundary curves, it is found that there is a trade-off between time switching scheme and power splitting scheme. When R_1 is small, the achievable rate of UE 2 in time switching scheme is larger than that in power splitting scheme. When R_2 is large, the relation reverses. In addition, the *cut-off* line in time switching scheme is shown in the figure, i.e., any point on the right side of line $R_1 = \frac{\xi|h_1|^2 P_{\max}}{\xi|h_1|^2 P_{\max} + P_{\mathrm{SIC}}} \log_2\left(1 + \frac{|h_1|^2 P_{\max}}{\sigma^2}\right)$ is not achievable.

In Fig. 3, the parameters are set to satisfy $|h_2|^2 > |h_1|^2 - \frac{P_{\mathrm{SIC}}}{\xi P_{\max}} > 0$. It can be seen that the boundary curves for time switching scheme and generalized scheme overlaps when $R_1 \leq \frac{\xi|h_1|^2 P_{\max}}{\xi|h_1|^2 P_{\max} + P_{\mathrm{SIC}}} \log_2\left(1 + \frac{|h_1|^2 P_{\max}}{\sigma^2}\right)$, which means that $\rho = 0$ is optimal. The reason is that in this condition, the decoding ability of UE 1 becomes the bottleneck, i.e., R_2 is constrained by the maximum supportable rate of UE 2' signal decoding in UE 1. Hence, all the received power should be split for information decoding in the second sub-slot in order to get a higher SINR. Also, the boundary curve for power splitting scheme forms a straight line, which is consistent with our analysis as Theorem 2. It is necessary to point out that when R_1 approaches zero, the gap between power splitting scheme and generalized scheme does not disappear. It is also due to the decoding bottleneck of UE 1 as splitting the received power for energy harvesting degrades the achievable rate of UE 2.

Further, the infeasible case for power splitting (i.e., $|h_1|^2 < \frac{P_{\mathrm{SIC}}}{\xi P_{\max}}$) is illustrated in Fig. 4. In this case, the achievable rate region of power splitting scheme becomes a straight line with

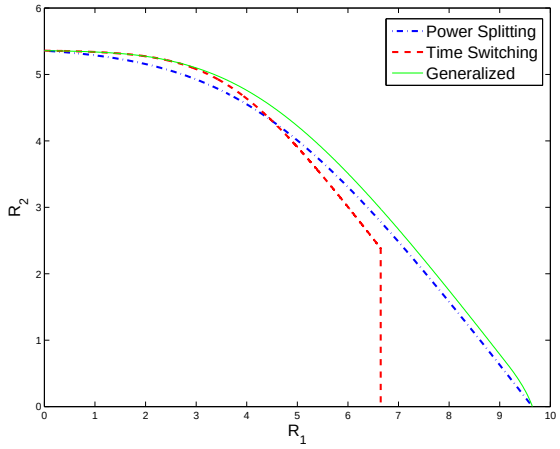

Fig. 2. Achievable rate regions of power splitting scheme, time switching scheme and generalized scheme with constant decoding power $P_{\mathrm{SIC}} = 160$mW. $P_{\max} = 40$W, $\sigma^2 = 0.1$mW, $\frac{|h_1|^2}{\sigma^2} = 20$dB, $\frac{|h_2|^2}{\sigma^2} = 0$dB, $\xi = 0.5$.

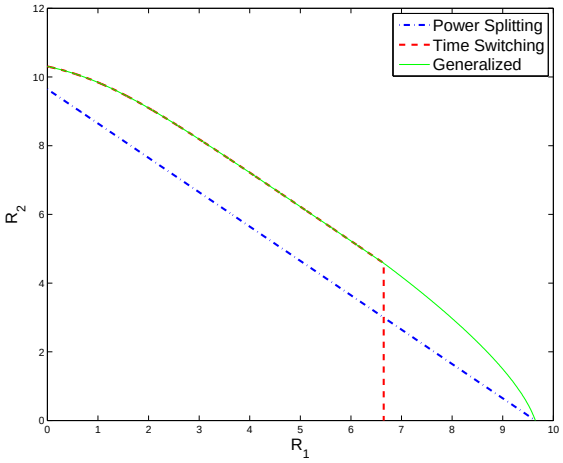

Fig. 3. Achievable rate regions of power splitting scheme, time switching scheme and generalized scheme with constant decoding power $P_{\mathrm{SIC}} = 160$mW. $P_{\max} = 40$W, $\sigma^2 = 0.1$mW, $\frac{|h_1|^2}{\sigma^2} = 20$dB, $\frac{|h_2|^2}{\sigma^2} = 15$dB, $\xi = 0.5$.

$R_1 = 0$. It can been seen that there is also a *cut-off* line for the achievable rate region of generalized scheme. Since pure power splitting scheme is infeasible, the existence of this line comes from the nature of time switching scheme, i.e., t is strictly larger than 0. The *cut-off* line can be expressed as $R_1 = \max_{0 \le t \le 1} f_1(t)$.

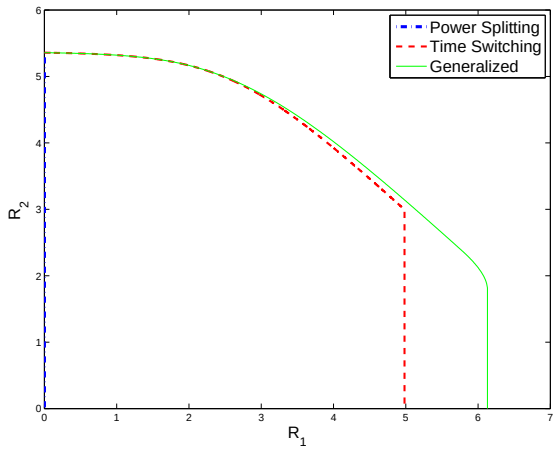

Fig. 4. Achievable rate regions of power splitting scheme, time switching scheme and generalized scheme with constant decoding power $P_{\mathrm{SIC}} = 160$mW. $P_{\max} = 40$W, $\sigma^2 = 0.1$mW, $\frac{|h_1|^2}{\sigma^2} = 18$dB, $\frac{|h_2|^2}{\sigma^2} = 0$dB, $\xi = 0.5$.

IV. Dynamic Decoding Power Consumption Case

In the previous section, we have studied constant power consumption model for information decoding. It is also necessary to consider dynamic decoding power consumption as the relation between decoding performance and number of iterations (proportional to decoding power consumption) has been found. For instance, an iterative decoding method for LDPC code was studied in [22, Fig. 8]. It is shown that to achieve the same error rate, the number of iterations is reduced with the increase of E_b/N_0, which corresponds to the decrease of information rate under a fixed SNR. Based on this, in this section, the decoding power consumption is modeled as an increasing function of information rate. It is expected to help enlarge the achievable rate region. Take power splitting scheme as an example, the stringent requirement on h_1 can be loosen under the dynamic power model, as one can reduce the required decoding power by sacrificing some rate. When dynamic decoding power model is considered, the equality conditions (see Lemma 1) may not be hold any more. Consequently, the problem becomes more complex and we propose an exhaustive search algorithm to find the achievable rate region.

A. Dynamic Power Model and Problem Formulation

As shown in [23, Theorem 1], the decoding energy consumption is lower-bounded as

$$P_{\mathrm{DEC}} \geq \frac{\omega R}{\sqrt{-\log_2(2p_e)}}, \tag{39}$$

where ω is a constant parameter related to circuit technology and coding block length, R is the information rate, and P_e is the symbol error rate, which is a function of SINR γ. Specifically, the symbol error rate for BPSK is expressed as

$$p_e = Q(\sqrt{\gamma}) = \int_{\sqrt{\gamma}}^{+\infty} \frac{1}{\sqrt{2\pi}} e^{-\frac{x^2}{2}} \mathrm{d}x. \tag{40}$$

In this paper, we use BPSK as an example, and the analysis can be easily extended to other modulation schemes. We approximate the decoding power consumption by the lower bound, and the total power consumption of UE 1 is modeled as

$$P_{\mathrm{SIC}} = \frac{\omega R_1^{(2)}}{\sqrt{-\log_2(2Q(\sqrt{\gamma_1}))}} + \frac{\omega R_2^{(2)}}{\sqrt{-\log_2(2Q(\sqrt{\gamma_2}))}} + P_r, \tag{41}$$

where P_r is the constant power consumption of analog receive circuit including filter, low noise amplifier, analog-to-digital converter and so on [10], and

$$\gamma_1 = \frac{|h_1|^2(1-\rho)P_1^{(2)}}{\sigma^2}, \tag{42}$$

$$\gamma_2 = \frac{|h_1|^2(1-\rho)P_2^{(2)}}{|h_1|^2(1-\rho)P_1^{(2)} + \sigma^2}. \tag{43}$$

Different from the constant decoding power case, not all the equality conditions in Lemma 1 hold in dynamic decoding power case. Nevertheless, by carefully checking the conditions, some constraints are still satisfied with equality.

Lemma 7. ***(Equality Constraints)*** *When the maximum of problem (*$\mathbf{P0}$*) with dynamic power model (41) is achieved, the constraints (3), (4), and (5) are satisfied with equality.*

Proof. See Appendix D. □

Based on Lemma 7, the original problem ($\mathbf{P0}$) can be reformulated as

$$(\mathbf{P4}) \quad \max \ t\log_2\left(1+\frac{|h_2|^2 P_{\max}}{\sigma^2}\right) + (1-t)R_2^{(2)} \tag{44a}$$

$$\text{s.t.} \ \ \log_2(1+\gamma_1) \geq \frac{r}{1-t}, \tag{44b}$$

$$R_2^{(2)} \leq \min\left\{R_{2,1}, R_{2,2}\right\}, \tag{44c}$$

$$\xi|h_1|^2 P_{\max}\left(\frac{t}{1-t}+\rho\right) \geq \frac{\omega r}{(1-t)\sqrt{-\log_2(2Q(\sqrt{\gamma_1}))}} + \frac{\omega R_2^{(2)}}{\sqrt{-\log_2(2Q(\sqrt{\gamma_2}))}} + P_r, \tag{44d}$$

$$0 \leq t < 1, 0 \leq \rho < 1, \tag{44e}$$

where γ_1 and γ_2 are expressed as (42) and (43), respectively, $P_2^{(2)} = P_{\max} - P_1^{(2)}$, and

$$R_{2,1} = \log_2\Big(1 + \frac{|h_1|^2(1-\rho)P_2^{(2)}}{|h_1|^2(1-\rho)P_1^{(2)} + \sigma^2}\Big), \tag{45}$$

$$R_{2,2} = \log_2\Big(1 + \frac{|h_2|^2 P_2^{(2)}}{|h_2|^2 P_1^{(2)} + \sigma^2}\Big). \tag{46}$$

Notice that the constraint (44d) can be rewritten as

$$R_2^{(2)} \le \frac{\sqrt{-\log_2(2Q(\sqrt{\gamma_2}))}}{\omega}\left(\xi|h_1|^2 P_{\max}\Big(\frac{t}{1-t}+\rho\Big) - \frac{\omega r}{(1-t)\sqrt{-\log_2(2Q(\sqrt{\gamma_1}))}} - P_r\right) \overset{def}{=} R_{2,\mathrm{P}}. \tag{47}$$

Thus, the optimal value of $R_2^{(2)}$ can be represented by t, ρ, and $P_1^{(2)}$, $R_2^{(2)} = \min\{R_{2,\mathrm{P}}, R_{2,1}, R_{2,2}\}$, i.e., it equals to the minimum between the values on the right hand side of constraints (44c) and (47). As a consequence, the optimization variables only include t, ρ, and $P_1^{(2)}$.

Due to the existence of Q function in the power constraint (44d), the relation between the optimization variables and the objective function is analytically intractable. Nevertheless, the optimal solution can be found by exhaustive search algorithm, which is detailed in the following subsection.

B. Exhaustive Search Algorithm

The intuitive way of exhaustive search is to search over the whole regions $\{(t, \rho, P_1^{(2)}) \big| 0 \le t < 1, 0 \le \rho < 1, 0 \le P_1^{(2)} \le P_{\max}\}$. If a variable vector $(t, \rho, P_1^{(2)})$ satisfies all the constraints and achieves the maximum of the objective, it is the optimal solution. In fact, the search range can be narrowed by exploring the monotonicity of (44b) with respect to each of the optimization variables.

Specifically, for a given target $r \in \Big[0, \log_2\big(1 + \frac{|h_1|^2 P_{\max}}{\sigma^2}\big)\Big]$, we have

$$t \le 1 - \frac{r}{\log_2\big(1 + \frac{|h_1|^2(1-\rho)P_1^{(2)}}{\sigma^2}\big)} \le 1 - \frac{r}{\log_2\big(1 + \frac{|h_1|^2 P_{\max}}{\sigma^2}\big)} \overset{def}{=} t_{\max}. \tag{48}$$

So the search range of t can be restricted to $t \in [0, t_{\max}]$. Once both r and t are given, we have

$$\rho \le 1 - \frac{\sigma^2}{|h_1|^2 P_1^{(2)}}\big(2^{\frac{r}{1-t}} - 1\big) \le 1 - \frac{\sigma^2}{|h_1|^2 P_{\max}}\big(2^{\frac{r}{1-t}} - 1\big) \overset{def}{=} \rho_{\max}. \tag{49}$$

Hence, the search range of ρ can be restricted to $\rho \in [0, \rho_{\max}]$. In addition, for given r, t and ρ, we have

$$P_1^{(2)} \ge \frac{\sigma^2}{|h_1|^2(1-\rho)}\big(2^{\frac{r}{1-t}} - 1\big) \overset{def}{=} P_{\min}. \tag{50}$$

Therefore, the search range of $P_1^{(2)}$ can be restricted to $P_1^{(2)} \in [P_{\min}, P_{\max}]$. In the restricted search range, the constraint (44b) is automatically satisfied. Then we only need to check if the right hand side of (47), $R_{2,\mathrm{P}}$, is nonnegative. The exhaustive search algorithm is summarized in Algorithm 2.

Algorithm 2 Exhaustive Search Algorithm

Input: $h_1, h_2, R_1 = r$

Output: R_2

Initialize $R_2 = 0$.
for all $t = 0, \delta t, 2\delta t, \cdots, \lfloor \frac{t_{\max}}{\delta t} \rfloor \delta t$ **do**
  for all $\rho = 0, \delta\rho, 2\delta\rho, \cdots, \lfloor \frac{\rho_{\max}}{\delta\rho} \rfloor \delta\rho$ **do**
    for all $P_1^{(2)} = P_{\min}, P_{\min} + \delta P, P_{\min} + 2\delta P, \cdots, P_{\min} + \lfloor \frac{P_{\max} - P_{\min}}{\delta P} \rfloor \delta P$ **do**
      Calculate $R_{2,\mathrm{P}}$, $R_{2,1}$, and $R_{2,2}$ according to (47), (45), and (46), respectively.
      if $R_{2,\mathrm{P}} \geq 0$ **then**
        Calculate $R_{2,\mathrm{temp}} = t \log_2 \left(1 + \frac{|h_2|^2 P_{\max}}{\sigma^2}\right) + (1-t) \min\{R_{2,1}, R_{2,2}, R_{2,\mathrm{P}}\}$.
        if $R_{2,\mathrm{temp}} > R_2$ **then**
          Update $R_2 = R_{2,\mathrm{temp}}$.
        end if
      end if
    end for
  end for
end for

Notice that t, ρ and $P_1^{(2)}$ are continuous variables. To computationally search over the feasible ranges, the feasible regions are discretized by step sizes δt, $\delta\rho$, and δP in the algorithm. The selection of the step sizes determines overall search time and search accuracy. The operation $\lfloor x \rfloor$ denotes the maximum integer no larger than x.

In addition, the exhaustive search algorithm can be easily extended to the special cases: time switching and power splitting, by simply restricting $\rho = 0$ or $t = 0$ to narrow the search range. With the proposed search algorithm, the achievable rate regions of generalized scheme, time switching scheme and power splitting scheme can be obtained, which are discussed in the following subsection.

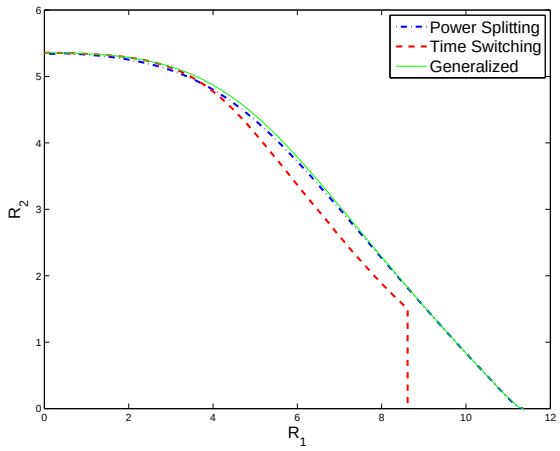

Fig. 5. Achievable rate regions of power splitting scheme, time switching scheme and generalized scheme with dynamic decoding power under parameters $P_r = 60$mW, $\omega = 0.044$. $P_{\max} = 40$W, $\sigma^2 = 0.1$mW, $\frac{|h_1|^2}{\sigma^2} = 20$dB, $\frac{|h_2|^2}{\sigma^2} = 0$dB, $\xi = 0.5$.

C. Achievable Rate Regions and Discussions

In this section, the achievable rate regions of generalized scheme, time switching scheme and power splitting scheme are depicted. The constant power consumption is $P_r = 60$mW, and the weight is set to $\omega = 0.044$ so that the maximum decoding power consumption does not exceed 160mW. The other parameters are consistent with those in Section III-D. Specifically, the parameters in Fig. 5 are the same with those in Fig. 2, the parameters in Fig. 6 are the same with those in Fig. 3, and the parameters in Fig. 7 are the same with those in Fig. 4.

It can be seen that the relation among the curves in Fig. 5 is similar with that in Fig. 2. The difference is that the regions are expanded towards R_1-axis. This is due to the reduction of decoding power consumption by tuning the achievable rates. It is also worth noting that the achievable rate region for power splitting scheme is very close to that for generalized scheme. The reason is that when the link quality between BS and UE 1 is sufficiently good, allocating more resources (time) to this link will benefit the overall performance as UE 1 can flexibly adjust rate and power consumption.

In Fig. 6, the boundary curve for power splitting scheme is no longer linear. The achievable region is expanded when R_1 is either much larger or much smaller than R_2. In this sense, the power splitting scheme is obviously not optimal, as one can get a larger achievable rate region by time sharing shown by the dotted line. This phenomenon results from the non-convexity of

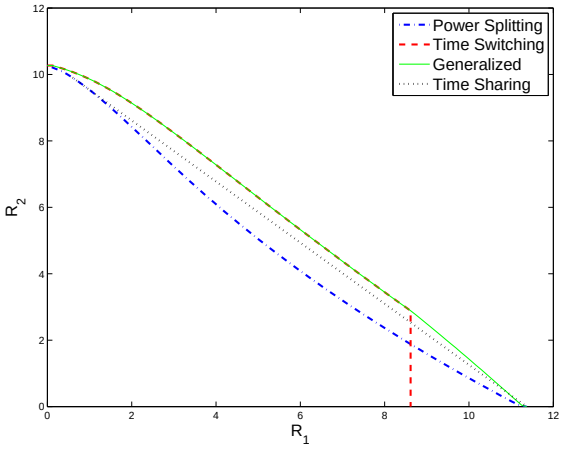

Fig. 6. Achievable rate regions of power splitting scheme, time switching scheme and generalized scheme with dynamic decoding power under parameters $P_r = 60$mW, $\omega = 0.044$. $P_{\max} = 40$W, $\sigma^2 = 0.1$mW, $\frac{|h_1|^2}{\sigma^2} = 20$dB, $\frac{|h_2|^2}{\sigma^2} = 15$dB, $\xi = 0.5$.

the problem $(\mathbf{P4})$.

Finally, as shown in Fig. 7, the power splitting scheme under dynamic power consumption model is feasible even when the link quality between BS and UE 1 is not good enough. In this case, the decoding power consumption can be reduced by decreasing the information rate to meet the available harvested energy. However, the user fairness performance is poor, i.e., if one of the users is served with high data rate, the other will experience very low data rate as more power is allocated to the former user, and more harvested energy is used to decode its information. Thus, the gap between the power splitting scheme and the generalized scheme is small when either R_1 or R_2 approaches its maximum, while the largest gap appears around the line $R_1 = R_2$.

V. Extended Results and Comparison

In this section, extended numerical results are presented to compare the achievable regions with the change of power consumption. We fix the parameters $\omega = 0.044$, $P_{\max} = 40$W, $\sigma^2 = 0.1$mW, $\frac{|h_1|^2}{\sigma^2} = 20$dB, $\frac{|h_2|^2}{\sigma^2} = 0$dB, $\xi = 0.5$, and change the values of P_{SIC} and P_r. Notice that when $\omega = 0.044$, the maximum power consumption for SIC decoding is approximately 100mW in our settings. Thus, if $P_{\text{SIC}} - P_r = 100$mW, the comparison between static power model and dynamic power model is fair.

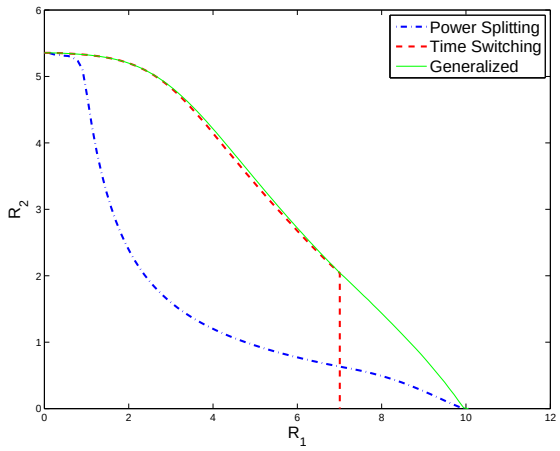

Fig. 7. Achievable rate regions of power splitting scheme, time switching scheme and generalized scheme with dynamic decoding power under parameters $P_r = 60$mW, $\omega = 0.044$. $P_{\max} = 40$W, $\sigma^2 = 0.1$mW, $\frac{|h_1|^2}{\sigma^2} = 18$dB, $\frac{|h_2|^2}{\sigma^2} = 0$dB, $\xi = 0.5$.

The performance comparison of generalized scheme is depicted in Fig. 8. It can be seen that comparable power consumption, the achievable rate region under dynamic power model is larger than that under static power model. In addition, as the information decoding power consumption increases, the rate regions shrink. It is worth noting that the direction of shrink is towards R_1-axis, i.e, R_1 becomes smaller as power consumption becomes larger. It illustrates the tradeoff between energy harvesting and information decoding. Furthermore, only the curve with static power $P_{\text{SIC}} = 200$mW has a cut-off line since $\xi|h_1|^2 P_{\max} = 200$mW. It can be predicted that if $P_r \geq 200$mW, there is also a cut-off line on the curve with dynamic power model.

In Fig. 9, it is shown that the achievable rate regions of time switching scheme are of the same shape, i.e., there is always a cut-off line. In addition, as the constant power consumption increases, the difference between the cut-off lines under static power model and dynamic power model becomes small.

Finally, the performance comparison of power splitting scheme is shown in Fig. 10. Different from generalized scheme and time switching scheme, with the increase of power consumption, the achievable rate region of power splitting scheme shrinks from the "middle" of the region. That is, the fairness between the two users can not be guaranteed.

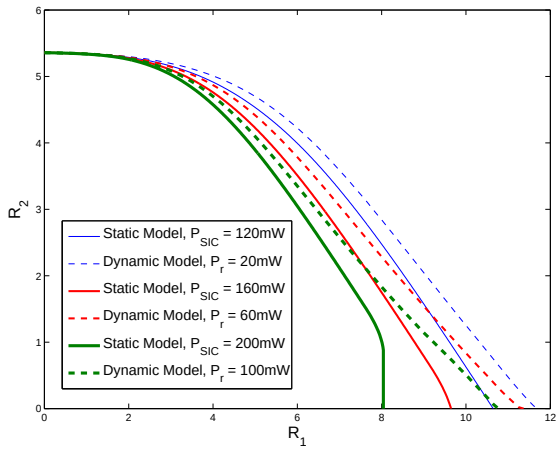
Static Model, P_SIC = 120mW
Dynamic Model, P_r = 20mW
Static Model, P_SIC = 160mW
Dynamic Model, P_r = 60mW
Static Model, P_SIC = 200mW
Dynamic Model, P_r = 100mW
R_1
R_2

Fig. 8. Achievable rate regions of generalized scheme with constant and dynamic decoding power. $\omega = 0.044$, $P_{\max} = 40$W, $\sigma^2 = 0.1$mW, $\frac{|h_1|^2}{\sigma^2} = 20$dB, $\frac{|h_2|^2}{\sigma^2} = 0$dB, $\xi = 0.5$.

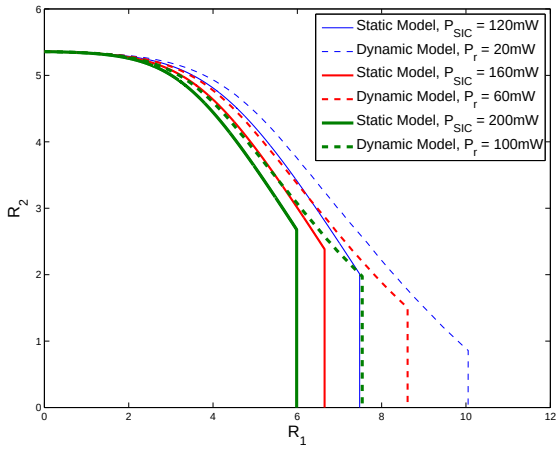
Static Model, P_SIC = 120mW
Dynamic Model, P_r = 20mW
Static Model, P_SIC = 160mW
Dynamic Model, P_r = 60mW
Static Model, P_SIC = 200mW
Dynamic Model, P_r = 100mW
R_1
R_2

Fig. 9. Achievable rate regions of time switching scheme with constant and dynamic decoding power. $\omega = 0.044$, $P_{\max} = 40$W, $\sigma^2 = 0.1$mW, $\frac{|h_1|^2}{\sigma^2} = 20$dB, $\frac{|h_2|^2}{\sigma^2} = 0$dB, $\xi = 0.5$.

VI. Conclusions

In this paper, we characterized the achievable rate region of the NOMA system with wireless powered near user. A generalized energy harvesting scheme combining the conventional time switching scheme and power splitting scheme was proposed. Under constant decoding power model, the proposed scheme is shown to enlarge the rate region compared with conventional schemes. The special cases: time switching and power splitting are of closed-form expressions

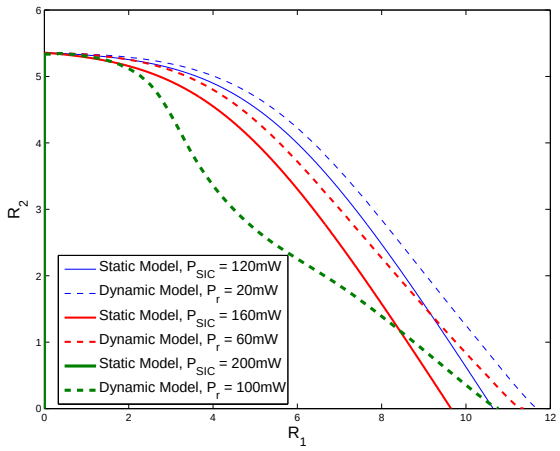
Static Model, P_SIC = 120mW
Dynamic Model, P_r = 20mW
Static Model, P_SIC = 160mW
Dynamic Model, P_r = 60mW
Static Model, P_SIC = 200mW
Dynamic Model, P_r = 100mW
R_1
R_2

Fig. 10. Achievable rate regions of power splitting scheme with constant and dynamic decoding power. $\omega = 0.044$, $P_{\max} = 40$W, $\sigma^2 = 0.1$mW, $\frac{|h_1|^2}{\sigma^2} = 20$dB, $\frac{|h_2|^2}{\sigma^2} = 0$dB, $\xi = 0.5$.

for the maximum achievable rates. Hence, the structure of the achievable region can be explicitly described. Specifically, there exists a cut-off line on the boundary of the rate region for time switching scheme, and that for power splitting scheme is linear if $|h_2|^2 \geq |h_1|^2 - \frac{P_{\text{SIC}}}{\xi P_{\max}}$. In addition, if $|h_1|^2 \leq \frac{P_{\text{SIC}}}{\xi P_{\max}}$, UE 1 can not be self powered on, and hence, the power splitting scheme is not feasible. Under dynamic decoding power model, the rate region is further expanded with efficient rate-dependent information decoder. Also, the barrier for applying power splitting scheme, i.e., the feasibility requirement on h_1 is broken. UE 1 can support a low rate transmission with reduced decoding power consumption. However, the fairness between users are sacrificed, i.e., the harvested energy is not sufficient to simultaneously support high data rate for both users.

APPENDIX A
PROOF OF LEMMA 1

Since $R_2^{(1)}$ is only constrained by (4), and $R_2^{(2)}$ is constrained by both (7) and (8), it is obvious that equality in (4) and (7) (or (8)) should be satisfied for maximization.

The equality of the power constraints (3) and (5) can be proved by contradiction. Take (3) as an example, assume that $P_2^{(1)} < P_{\max}$ achieves the maximum average rate, we consider a value $\hat{P}_2^{(1)}$ that satisfies $P_2^{(1)} < \hat{P}_2^{(1)} \leq P_{\max}$. It does not violate the decoding power constraint (9). With $\hat{P}_2^{(1)}$, we can achieve a higher rate for the first sub-slot $R_2^{(1)}$, and hence a higher average

rate $tR_2^{(1)}+(1-t)R_2^{(2)}$. It contradicts the optimality assumption of $P_2^{(1)}$. The equality of (5) can be proved similarly.

Given the condition that (3)-(5) and (7) (or (8)) are satisfied with equality, the objective (11a) is an decreasing function of $P_1^{(2)}$. As $P_1^{(2)}$ is lower bounded by (6), the objective is minimized when (6) is satisfied with equality.

APPENDIX B
PROOF OF LEMMA 3

Denote $\alpha=\log_2\left(1+\frac{|h_2|^2P_{\max}}{\sigma^2}\right), \beta=\frac{|h_2|^2}{|h_1|^2}$ for simplicity. As $0<|h_2|^2<|h_1|^2$ by assumption, we have $0<\beta<1$. Then $f_0(t)$ can be rewritten as

$$f_0(t)=\alpha-(1-t)\log_2(\beta 2^{\frac{r}{1-t}}+1-\beta). \tag{51}$$

The first derivative of $f_0(t)$ at $t=0$ is

$$\begin{aligned} f_0'(0)=&\Big[\log_2(\beta 2^{\frac{r}{1-t}}+1-\beta)-\frac{\beta r 2^{\frac{r}{1-t}}}{(1-t)(\beta 2^{\frac{r}{1-t}}+1-\beta)}\Big]\Big|_{t=0}\\ =&\frac{(\beta 2^r+1-\beta)\log_2(\beta 2^r+1-\beta)-\beta r 2^r}{\beta 2^r+1-\beta}. \end{aligned} \tag{52}$$

Denote

$$g(\beta)=(\beta 2^r+1-\beta)\log_2(\beta 2^r+1-\beta)-\beta r 2^r, \tag{53}$$

we have

$$g''(\beta)=\frac{(2^r-1)^2}{(\beta 2^r+1-\beta)\ln 2}\geq 0, \tag{54}$$

which indicates that $g(\beta)$ is a convex function of β. Therefore, the maximum of $g(\beta)$ is achieved at the boundary points, i.e.,

$$g(\beta)\leq \max\{g(0),g(1)\}=0. \tag{55}$$

Hence, we have

$$f_0'(0)=\frac{g(\beta)}{\beta 2^r+1-\beta}\leq 0. \tag{56}$$

Notice that the second derivative of function $f_0(t)$ satisfies

$$f_0''(t)=-\frac{\beta(1-\beta)r^2 2^{\frac{r}{1-t}}\ln 2}{(1-t)^3(\beta 2^{\frac{r}{1-t}}+1-\beta)^2}\leq 0, \tag{57}$$

i.e., the first derivative $f_0'(t)$ is non-increasing. Consequently,

$$f_0'(t)\leq f_0'(0)\leq 0,\ \forall 0\leq t<1, \tag{58}$$

which means that $f_0(t)$ is a non-increasing function.

APPENDIX C
PROOF OF LEMMA 5

Denote $\alpha = \log_2\left(1+\frac{|h_2|^2 P_{\max}}{\sigma^2}\right), \beta = \frac{|h_2|^2}{|h_1|^2}, \zeta = \frac{P_{\text{SIC}}}{\xi|h_1|^2 P_{\max}}$ for simplicity. The function can be rewritten as

$$f_2(t) = \alpha - (1-t)\log_2\Big(\frac{\beta}{\frac{1}{1-t}-\zeta}\big(2^{\frac{r}{1-t}}-1\big)+1\Big). \tag{59}$$

Define

$$g_1(x) = \log_2\Big(\frac{\beta}{x-\zeta}\big(2^{rx}-1\big)+1\Big). \tag{60}$$

As $f_2(t) = \alpha - (1-t)g(\frac{1}{1-t})$, according to the property of perspective of a function [20, Example 3.20], to prove the concavity of $f_2(t)$, it is equivalent to prove the convexity of $g_1(x)$ for $x > \zeta$. Further more, denote

$$g_2(x) = \frac{\beta}{x-\zeta}\big(2^{rx}-1\big)+1. \tag{61}$$

We can rewrite that

$$g_1(x) = -\log_2\frac{1}{g_2(x)}. \tag{62}$$

According to the convexity of function composition [20, Eq. (3.11)], as $-\log_2 x$ is convex and decreasing for $x > 0$, $g_1(x)$ is convex if $\frac{1}{g_2(x)}$ is concave. Again, as $-\frac{1}{x}$ is concave and increasing for $x < 0$, $\frac{1}{g_2(x)}$ is concave if $-g_2(x)$ is concave. Therefore, to prove the convexity of $g_1(x)$, it is equivalent to prove the convexity of $g_2(x)$.

By taking the second derivative of $g_2(x)$, we have

$$g_2''(x) = \frac{\beta}{(x-\zeta)^3}\Big(2^{rx}\big((r(x-\zeta)\ln 2-1)^2+1\big)-2\Big). \tag{63}$$

Then denote

$$g_3(x) = 2^{rx}\big((r(x-\zeta)\ln 2-1)^2+1\big)-2. \tag{64}$$

Since

$$g_3'(x) = 2^{rx}(r\ln 2)^3(x-\zeta)^2 > 0, \tag{65}$$

$g_3(x)$ is an increasing function. We discuss the sign of $g_2''(x)$ for two cases.

(a): If $P_{\text{SIC}} < \xi|h_1|^2 P_{\max}$, i.e., $0 < \zeta < 1$. Therefore, we have $x - \zeta > 0$ and

$$g_3(x) \geq g_3(1) = 2^r\big((r(1-\zeta)\ln 2-1)^2+1\big)-2 \overset{def}{=} g_4(r). \tag{66}$$

Again, we have

$$g_4'(r) = 2^r \ln 2\big((r(1-\zeta)\ln 2 - \zeta)^2 + 1 - (1-\zeta)^2\big) > 0, \tag{67}$$

based on which we have $g_4(r) \geq g_4(0) = 0$. It means that $g_3(x) \geq 0$, and hence $g_2''(x) \geq 0$ for all $x > 1$.

(b): If $P_{\rm SIC} \geq \xi|h_1|^2 P_{\max}$ and $1 - \frac{\xi|h_1|^2 P_{\max}}{P_{\rm SIC}} < t < 1$, we have $x > \zeta \geq 1$. Hence, $g_3(x) > g_3(\zeta) = 2(2^{r\zeta} - 1) > 0$, which again, guarantees that $g_2''(x) \geq 0$. As a result, $g_2(x)$ is convex, and hence, the lemma is proved.

APPENDIX D
PROOF OF LEMMA 7

The equality of (3) and (4) is the same as Lemma 1. We now prove the equality of (5) by contradiction.

Suppose the strict inequality holds in (5). Since $Q(\sqrt{\gamma_2})$ is a decreasing function of γ_2, it is also a decreasing function of $P_2^{(2)}$. Hence, $\sqrt{-\log_2(2Q(\sqrt{\gamma_2}))}$ is an increasing function of $P_2^{(2)}$. By properly increasing $P_2^{(2)}$ and $R_2^{(2)}$ so that the right hand side of (9) keeps fixed, we can obtain a higher average rate without violating any constraints. It contradicts the optimality assumption, and hence, (5) must be satisfied with equality.

REFERENCES

[1] L. Dai, B. Wang, Y. Yuan, S. Han, C. l. I, and Z. Wang, "Non-orthogonal multiple access for 5g: solutions, challenges, opportunities, and future research trends," *IEEE Communications Magazine*, vol. 53, no. 9, pp. 74–81, Sept. 2015.

[2] Y. Saito, Y. Kishiyama, A. Benjebbour, T. Nakamura, A. Li, and K. Higuchi, "Non-orthogonal multiple access (noma) for cellular future radio access," in *IEEE Vehicular Technology Conference (VTC Spring)*, Jun. 2013, pp. 1–5.

[3] S. Bi, Y. Zeng, and R. Zhang, "Wireless powered communication networks: an overview," *IEEE Wireless Communications*, vol. 23, no. 2, pp. 10–18, Apr. 2016.

[4] Y. Saito, A. Benjebbour, Y. Kishiyama, and T. Nakamura, "System-level performance evaluation of downlink non-orthogonal multiple access (noma)," in *IEEE International Symposium on Personal, Indoor, and Mobile Radio Communications (PIMRC)*, Sept. 2013, pp. 611–615.

[5] M. Al-Imari, P. Xiao, M. A. Imran, and R. Tafazolli, "Uplink non-orthogonal multiple access for 5g wireless networks," in *IEEE International Symposium on Wireless Communications Systems (ISWCS)*, Aug. 2014, pp. 781–785.

[6] S. Timotheou and I. Krikidis, "Fairness for non-orthogonal multiple access in 5g systems," *IEEE Signal Processing Letters*, vol. 22, no. 10, pp. 1647–1651, Oct. 2015.

[7] Z. Ding, P. Fan, and H. V. Poor, "Impact of user pairing on 5g nonorthogonal multiple-access downlink transmissions," *IEEE Transactions on Vehicular Technology*, vol. 65, no. 8, pp. 6010–6023, Aug 2016.

[8] Z. Ding, M. Peng, and H. V. Poor, "Cooperative non-orthogonal multiple access in 5g systems," *IEEE Communications Letters*, vol. 19, no. 8, pp. 1462–1465, Aug. 2015.

[9] Y. Liu, Z. Ding, M. Elkashlan, and H. V. Poor, "Cooperative non-orthogonal multiple access with simultaneous wireless information and power transfer," *IEEE Journal on Selected Areas in Communications*, vol. 34, no. 4, pp. 938–953, Apr. 2016.

[10] S. Cui, A. J. Goldsmith, and A. Bahai, "Energy-constrained modulation optimization," *IEEE Transactions on Wireless Communications*, vol. 4, no. 5, pp. 2349–2360, Sept. 2005.

[11] S. Zhou, T. Chen, W. Chen, and Z. Niu, "Outage minimization for a fading wireless link with energy harvesting transmitter and receiver," *IEEE Journal on Selected Areas in Communications*, vol. 33, no. 3, pp. 496–511, Mar. 2015.

[12] L. Liu, R. Zhang, and K.-C. Chua, "Wireless information and power transfer: a dynamic power splitting approach," *IEEE Transactions on Communications*, vol. 61, no. 9, pp. 3990–4001, Sept. 2013.

[13] X. Zhou, R. Zhang, and C. K. Ho, "Wireless information and power transfer: Architecture design and rate-energy tradeoff," *IEEE Trans. on Communications*, vol. 61, no. 11, pp. 4754–4767, Nov. 2013.

[14] R. Zhang and C. K. Ho, "Mimo broadcasting for simultaneous wireless information and power transfer," *IEEE Transactions on Wireless Communications*, vol. 12, no. 5, pp. 1989–2001, May 2013.

[15] X. Zhou, R. Zhang, and C. K. Ho, "Wireless information and power transfer in multiuser ofdm systems," *IEEE Transactions on Wireless Communications*, vol. 13, no. 4, pp. 2282–2294, Apr. 2014.

[16] G. Zhu, C. Zhong, H. A. Suraweera, G. K. Karagiannidis, Z. Zhang, and T. A. Tsiftsis, "Wireless information and power transfer in relay systems with multiple antennas and interference," *IEEE Transactions on Communications*, vol. 63, no. 4, pp. 1400–1418, Apr. 2015.

[17] K. Huang and V. K. Lau, "Enabling wireless power transfer in cellular networks: architecture, modeling and deployment," *IEEE Transactions on Wireless Communications*, vol. 13, no. 2, pp. 902–912, Feb. 2014.

[18] J. Park and B. Clerckx, "Joint wireless information and energy transfer in a two-user MIMO interference channel," *IEEE Transactions on Wireless Communications*, vol. 12, no. 8, pp. 4210–4221, Aug. 2013.

[19] S. Lee, L. Liu, and R. Zhang, "Collaborative wireless energy and information transfer in interference channel," *IEEE Transactions on Wireless Communications*, vol. 14, no. 1, pp. 545–557, Jan. 2015.

[20] S. P. Boyd and L. Vandenberghe, *Convex optimization*. Cambridge university press, 2004.

[21] L. Richard and J. Burden, *Numerical Analysis*. PWS Publishing Co., Boston, MA, 1985.

[22] Y. Kou, S. Lin, and M. P. C. Fossorier, "Low-density parity-check codes based on finite geometries: a rediscovery and new results," *IEEE Transactions on Information Theory*, vol. 47, no. 7, pp. 2711–2736, Nov 2001.

[23] C. G. Blake and F. R. Kschischang, "Energy consumption of VLSI decoders," *IEEE Transactions on Information Theory*, vol. 61, no. 6, pp. 3185–3198, Jun. 2015.